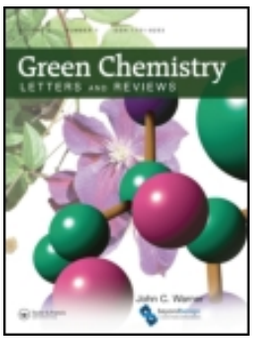

Green Chemistry Letters and Reviews

ISSN: 1751-8253 (Print) 1751-7192 (Online) Journal homepage: http://www.tandfonline.com/loi/tgcl20

An active and recyclable bicontinuous cubic Ia3d mesostructural Rh(I) organometal catalyst for 1,4-conjugate addition reaction in aqueous medium

Fengxia Zhu, Xiaojun Sun, Jianfeng Zhou & Pusu Zhao

To cite this article: Fengxia Zhu, Xiaojun Sun, Jianfeng Zhou & Pusu Zhao (2014) An active and recyclable bicontinuous cubic Ia3d mesostructural Rh(I) organometal catalyst for 1,4-conjugate addition reaction in aqueous medium, Green Chemistry Letters and Reviews, 7:3, 250-256, DOI: 10.1080/17518253.2014.922625

To link to this article: https://doi.org/10.1080/17518253.2014.922625

Published online: 21 Jul 2014.

Green Chemistry Letters and Reviews, 2014
Vol. 7, No. 3, 250–256, http://dx.doi.org/10.1080/17518253.2014.922625

Taylor & Francis
Taylor & Francis Group

RESEARCH LETTER

An active and recyclable bicontinuous cubic Ia3d mesostructural Rh(I) organometal catalyst for 1,4-conjugate addition reaction in aqueous medium

Fengxia Zhu[a,b], Xiaojun Sun[a], Jianfeng Zhou[a] and Pusu Zhao[a]*

[a]*Jiangsu Key Laboratory for Chemistry of Low-dimensional Materials, College of Chemistry and Chemical Engineering, Huaiyin Normal University, Huaian, Jiangsu, China;* [b]*Key Laboratory of Chemical Resources, Ministry of Education, Shanghai Normal University, Shanghai, China*

(*Received 20 November 2013; final version received 6 May 2014*)

An active and reusable heterogeneous Rh(I) organometal catalyst (Rh(I)-PMO-3D) was synthesized by template-directed co-condensation of $Rh[PPh_2(CH_2)_2Si(OCH_2CH_3)_3]_3Cl$ and $(CH_3CH_2O)_3SiPhSi(OCH_2CH_3)_3$. This catalyst displayed bicontinuous cubic Ia3d mesostructure channel, which ensured the high dispersion of Rh(I) active sites and the convenient diffusion of reactant molecules into the pore channels. Meanwhile, the Ph-functionalization could enhance the surface hydrophobicity, which promoted the adsorption of organic reactant molecules on the catalyst, especially in aqueous medium. During water-medium 1,4-conjugate addition reactions, Rh(I)-PMO-3D catalyst exhibits higher catalytic activity than the corresponding homogeneous Rh(I) catalyst and could be used repetitively for more than five times, showing a good potential in industrial applications.

Keywords: heterogenized Rh(I) organometallic catalyst; bicontinuous cubic mesostructure; 1,4-conjugate addition reaction; aqueous medium

Introduction

Carbon–carbon bond formation reaction is an indispensable powerful tool in organic synthesis, finding numerous applications in the preparation of pharmaceuticals and fine chemicals. The Rh-catalyzed 1,4-conjugate addition of reagents to acrylic α,β-unsaturated carbonyl compounds (enones) represents an important carbon–carbon forming reaction in organic chemistry (*1–3*).

In general, the reaction is conducted in organic solvent, which eventually adds to environmental problems (*4*). A notable development is the use of water and aqueous solvents as an alternative nonpolluting solvent for organic reactions because of their environmental friendliness. To date, most studies focused on homogeneous organometallic catalysts for water-medium 1,4-conjugate addition reaction due to the solubility limit (*5*). Although homogeneous catalysts work very well, their industrial applications are limited by both tedious work-up and non-trivial separation procedures, which may lead to contamination of the final product. In addition, homogeneous catalysts suffer from short lifetimes resulting in poor recyclability, which may increase cost and lead to heavy-metal pollution in water (*6*, *7*). Solid-supported homogeneous organometallic catalysts could effectively circumvent this issue. To obtain high catalytic efficiency matchable with that of the corresponding homogeneous catalysts, the as-prepared immobilized organometallic catalysts should maintain both the effective chemical environment and the high degree of dispersion of active sites.

Recent progress in functionalized mesoporous silica has highlighted the potential of utilizing these structurally uniform materials as a new generation of powerful heterogeneous catalysts (*8*, *9*). Among them, the three-dimensional (3D) cubic mesoporous organosilica material designated PMO-3D is now attracting wide interest owing to the great perspectives of application in catalysis (*10*). On one hand, the periodic mesoporous silicas (PMOs) with large surface area (*11–13*) provide a promising way for designing immobilized homogeneous catalysts with high efficiency owing to the uniform distribution of active sites (*14*). Meanwhile, functionalization with organic groups was also performed to enhance surface hydrophobicity, which promoted the diffusion and adsorption of organic molecules on the catalysts, especially in aqueous medium (*15–17*). On the other hand, this unique 3D interconnected network of PMO-3D provides a highly open porous host with an easy and

*Corresponding author. Email: zhaopusu66@sohu.com

direct access for organic molecules and facilitates inclusion or diffusion throughout the pore system without pore blockage. However, to our best knowledge, this 3D mesoporous organometalsilica with both the organometal rhodium and phenyl bridging groups incorporated into 3D mesoporous organosilica framework has never been reported so far. Herein, we report the synthesis of a 3D mesoporous organorhodium(I) silica catalyst with both Rh(I) organometals and rigid aromatic bridging groups (Ph) integrally incorporating into silica framework. This catalyst exhibits higher activity than the corresponding Rh(I) homogeneous catalyst and could be used repetitively in water-medium 1,4-conjugate addition reaction, showing a good potential in industrial applications.

Experimental

Catalyst preparation

Firstly, a Rh(I) organometallic silane was synthesized in an oxygen-free and dry argon atmosphere using Schlenk techniques (*18*). In a typical run of synthesis, 5.4 mL of 2-(diphenylphosphino)-ethyltriethoxysilane [$PPh_2CH_2CH_2Si(OCH_2CH_3)_3$] was added slowly into 30 mL of anhydrous toluene containing 1.0 g [Rh(COD)Cl]$_2$. After the solution was stirred for 24 h at room temperature, the toluene was evaporated and the viscous residue was dissolved in 50 mL of anhydrous hexane. After cooling to −40°C, dark red oil was obtained and then dried at 40°C under vacuum. The composition was determined as Rh[$PPh_2(CH_2)_2Si(OCH_2CH_3)_3]_3Cl$, which was confirmed by inductively coupled plasma (ICP) analysis and ^{1}H NMR (CD_2Cl_2) analysis: 7.1–7.4, 7.5–7.8 (3 m, 30 H, ArH), 3.6 (m, 18 H,OCH_2), 2.6 (m, 6 H, CH_2P), 1.1 (m, 27 H, CH_3), and 0.78 (m, 6 H, $SiCH_2$). Then, the periodic mesoporous organorhodium(I)silica with bicontinuous cubic Ia3d mesostructure, denoted as Rh(I)-PMO-3D, was prepared by co-condensation method. In a typical synthesis, 1.8 g of P123 was dissolved in 60 g of distilled water and 4.5 g of 2.0 M HCl solution with stirring at 35°C. After complete dissolution, 1.6 g of butanol was added at once. After stirring for 1 h, a certain amount of bis(triethoxysilyl) benzene ($(CH_3CH_2O)_3SiPhSi(OCH_2CH_3)_3$, BTEB) was added to the homogeneous solution. After being prehydrolyzed for 1 h, Rh[$PPh_2(CH_2)_2Si(OCH_2CH_3)_3]_3Cl$ was added into the solution. The initial molar ratio in the mother solution is Si:P123:butanol:HCl:H_2O = 1.0:0.068:4.9:2.0:800, where Si refers to the total silica source. This mixture was left under vigorous stirring at 35°C for 24 h. Subsequently, hydrothermal treatment of the reactant mixture was carried out at 100°C for 72 h under static conditions in a closed polypropylene bottle. Finally, the surfactants and other organic substances were extracted by refluxing in ethanol solution at 80°C for 24 h, leading to the Rh(I)-PMO-3D catalyst. The Rh(I) loading was adjusted by changing the amount of Rh[$PPh_2(CH_2)_2Si(OCH_2CH_3)_3]_3Cl$ in the initial mixture, corresponding to Rh(I)-PMO-3D-1, Rh(I)-PMO-3D-2, and Rh(I)-PMO-3D-3. According to ICP analysis, the real Rh(I) loadings in the three catalysts were determined as 0.44, 0.86, and 1.1wt%, respectively.

For comparison, the Rh(I)-PMO-2D, which 2D denotes two dimension, was also prepared according the method recorded by Li (*9*). Briefly, 0.42 g Rh[$PPh_2(CH_2)_2Si(OCH_2CH_3)_3]_3Cl$ in 1.0 mL of tetrahydrofuran was mixed with 40 mL of 0.20 M HCl aqueous solution containing 1.8 g of BTEB, 1.0 g of P123, and 3.0 g of KCl, which has been prehydrolyzed for 40 min at 40°C. After being stirred at the same temperature for 24 h and aged at 100°C for another 24 h, the precipitate was filtrated and dried under a vacuum overnight. Finally, the surfactants and other organic substances were removed by the above method, leading to the Rh(I)-PMO-2D catalyst. The Rh(I) loading was determined as 0.87 wt% by ICP analysis.

Characterization

The compositions and Rh(I) loadings were determined by elemental analysis (Elementar Vario ELIII, Germany) and inductively coupled plasma optical emission spectrometer (ICP-OES, Varian VISTA-MPX). Low-angle X-ray powder diffraction (XRD) patterns were obtained on a Rigaku D/maxr B diffractometer with Cu Ka. N_2 adsorption–desorption isotherms were measured at −196°C on a Quantachrome NOVA 4000e analyzer, from which the specific surface area (S_{BET}) was calculated by applying Brunauer–Emmett–Teller (BET) method and Barrett–Joyner–Halenda (BJH) model on the adsorption branches, respectively. Meanwhile, the average pore diameter (D_P) and total pore volume (V_P) were calculated from the adsorption isotherms using BJH model. Surface morphologies and porous structures were observed through a transmission electron microscopy (TEM, JEOL JEM2011). The surface electronic states were analyzed by X-ray photoelectron spectroscopy (XPS, Perkin-Elmer PHI 5000C). All the binding energy (BE) values were calibrated by using the standard BE value of contaminant carbon (C_{1S} = 284.6 eV) as a reference.

Activity test

The 1,4-conjugate addition reaction (Scheme 1) was used as probe to evaluate the catalytic performances of different catalysts, which was carried out in a

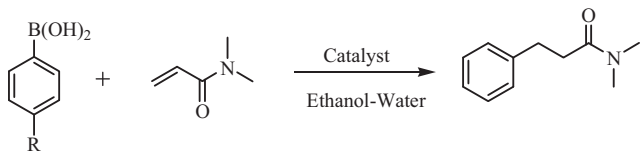

Scheme 1. The 1,4-conjugate addition reaction between phenylboronic acid and *N*,*N*-acrylic amide.

10-mL round-bottomed flask at 80°C under vigorous stirring. In a typical run of the reaction, 0.50 mmol of arylboronic acids, 0.10 mmol of *N*,*N*-acrylic amide, 1.0 mL of toluene, 4.0 mL H_2O, *n*-decane as an internal standard, and a catalyst containing 0.0065 mmol Rh(I) were mixed in the flask. After reaction for 7 h, the products were extracted by toluene, and followed by an analysis on a gas chromatograph (SHIMADZU, GC-17A) equipped with a JWDB-5, 95% dimethyl 1-(5%)-diphenylpolysiloxane column, and a flame ionization detector. The reproducibility was checked by repeating each result at least three times and is found to be within (±5%).

Recycling experiments

In order to determine the catalyst durability, the catalyst was allowed to centrifuge after each run of reactions and the clear supernatant liquid was decanted slowly. The catalyst was washed thoroughly with distilled water and ethanol. The solid material was subsequently dried and transferred to a reaction flask before employed in the next reaction (next recycling step). The same amounts and experimental procedure was adapted as used in a single reaction. The catalyst was stored under air atmosphere in between reactions.

Results and discussion

Structural characteristics

The presence of the organic moieties in the walls of the material was established by solid-state NMR investigations (Figure 1). The ^{29}Si MAS NMR spectrum revealed that the Rh(I)-PMO-3D displayed three signals at −62, −71 and −80 ppm corresponding to T^1 [$RSi(OSi)(OH)_2$], T^2 [$RSi(OSi)_2(OH)$], and T^3 [$RSi(OSi)_3$], respectively. No Q^n peaks were observed between −90 and −120 ppm, where Q^n = $Si(OSi)_n(OH)_{4-n}$, n = 2–4, indicating that all the Si species were covalently bonded with carbon atoms (*19*) during the acidic synthesis and extraction step. Meanwhile, two peaks around 14 and 32 ppm were observed in the ^{13}C CP MAS NMR spectrum, which could be assigned to two C atoms in the -CH_2-CH_2- group connecting with the PPh_2-group. An intense peak around 133 ppm could be attributable to the C atoms in the benzene ring (Ph) covalently bonded to the Si atoms. A weak

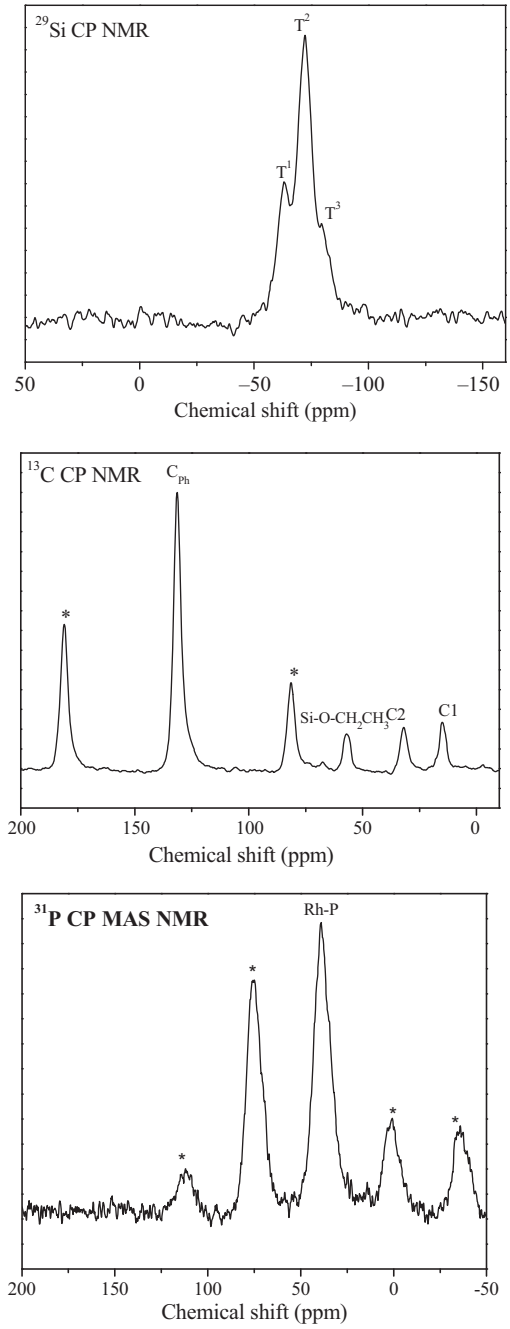

Figure 1. NMR spectra of the Rh(I)-PMO-3D sample.

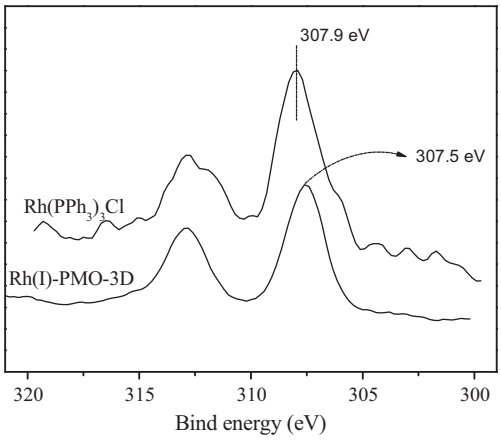

Figure 2. XPS spectra of the Rh(I)-PMO-3D sample.

peak around 59 ppm was assigned to the C atoms in the C_2H_5O-group connecting with silicon due to the incomplete hydrolysis of residual polymer templates (*20*). The resonances marked by asterisks are due to the spinning sidebands of benzene rings. In addition, the ^{31}P CP MAS NMR spectrum showed a single signal at 38 ppm, corresponding to P atom in the PPh_2-groups. The other peaks could be assigned to rotation side bands since their positions changed with the spinning speed (*21*). These results clearly demonstrated the integral incorporation of both the Rh(I) organometal and the Ph group into the silica framework.

As shown in Figure 2, the XPS spectra demonstrated that all the Rh species in the Rh(I)-PMO-3D were present in +1oxidation state (*22*), corresponding to the BE around 307.5 eV in $Rh_{3d5/2}$ level, which indicates that no phosphorus–rhodium bonds were cleaved during the synthesis of Rh(I)-PMO-3D. In comparison with free $Rh(PPh_3)_3Cl$ the Rh (I) BE in the Rh-PMO-3D shifted negatively by 0.4 eV, possibly due to the stronger electron-donating ability of P in the $PPh_2(CH_2CH_2)$ than that in the PPh_3, taking into account that $\prod$ conjugated system between P and three phenyl groups could dilute the electron density on the P atom.

Figure 3 revealed that the Rh(I)-PMO-3D displayed a typical IV type N_2 adsorption–desorption isotherm with a H_1 hysteresis loop indicative of the mesoporous structure (*23*). The low-angle XRD pattern showed an intense peak around 2 θ = 0.90° indicative of (211) and (220) diffraction and three additional weak peaks at higher 2 θ values corresponding to (220), (420), and (332) diffractions. These results demonstrated that the Rh(I)-PMO-3D contained ordered 3D mesoporous channels (*24*), which was further confirmed by TEM images (Figure 4). Some structural parameters including surface area (S_{BET}), pore diameter (D_P) and pore volume (V_P) were summarized in Table 1.

Catalytic performances

During the reaction, only the 2-arylethaneacylamides product was identified by GC–MS analysis, indicating that the catalysts were absolutely selective. Firstly, to confirm the location of the Rh(I) species incorporated into the mesoporous framework, the Rh(I)-PMO-3D catalyst was allowed to react with $KMnO_4$ in aqueous solution for enough time. The unreacted $KMnO_4$ was titrated quantitatively by $Na_2C_2O_4$. The Rh(I) content reacted with accessible catalytic $KMnO_4$ oxidation could be considered as these Rh(I) sites for catalytic reactions. The total Rh(I) species were determined by ICP analysis. The experimental results confirmed that the molar ratio between Rh(I) species determined by $KMnO_4$ oxidation and total Rh(I) species determined by ICP analysis was around 93%, suggesting that most of Rh(I) active sites in the Rh(I)-PMO-3D sample were accessible for catalytic reactions.

The effect of catalyst loading on conversion was also studied and the results are presented in Table 1. The control experiment indicated that the addition reaction did not occur in the absence of a catalyst, and the support PMO-3D was inert in the reaction. For the Rh(I)-PMO-3D series catalysts with different Rh(I) loadings, the catalytic activity first increased and then decreased with the increase in Rh(I) loading. The Rh(I)-PMO-3D-1 catalyst with very low Rh(I) loading exhibited poor activity due to the relatively long distance between the neighboring Rh(I) active sites. Taking into account that reaction needed two kinds of molecules adsorbed on the neighboring Rh(I) active sites, the big space between the neighboring Rh (I) active sites would not be in favor of intermolecular contact and has negative effect on the catalytic activity. Meanwhile, the Rh(I)-PMO-3D-3 with very high Rh(I) loading also showed poor activity, possibly due to the steric hindrance that retarded the diffusion and even the adsorption of organic molecules on the Rh(I) active sites. The Rh(I)-PMO-3D-2 with the Rh (I) loading was found to be optimum catalyst, which exhibited equivalent catalytic efficiencies with the corresponding $Rh(PPh_3)_3Cl$ homogeneous catalyst. The Rh(I)-PMO-3D-2 also showed higher catalytic activity than Rh(I)-PMO-2D with the similar Rh(I) loadings. This could be mainly attributed to this unique 3D interconnected network of PMO-3D, which provides a highly open porous host with an easy and direct access for organic molecules and facilitates inclusion or diffusion throughout the pore system without pore blockage.

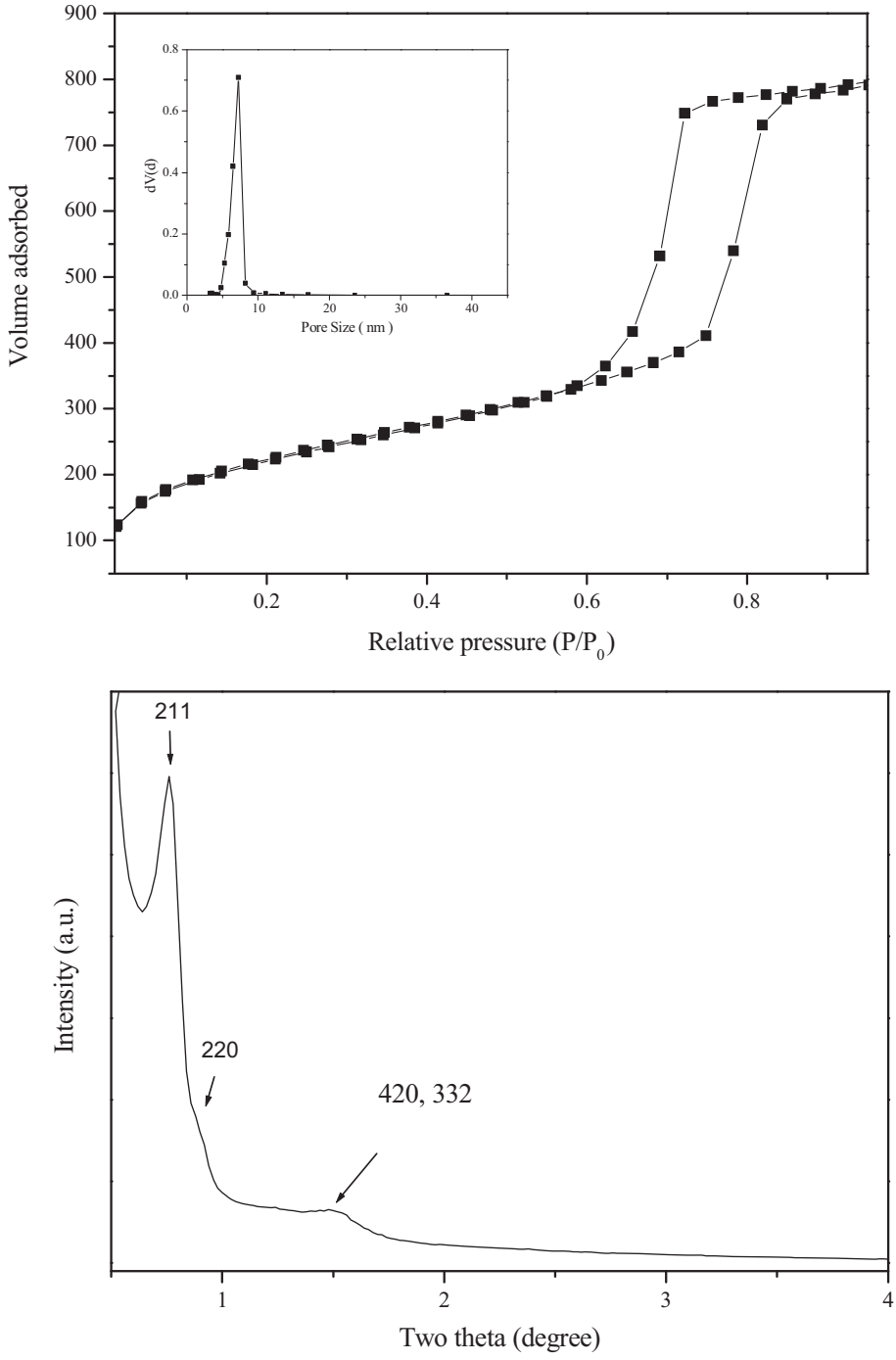

Figure 3. N_2 adsorption-desorption isotherms (up) and XRD pattern (down) of the Rh(I)-PMO-3D sample.

To evaluate the catalytic behaviors of the Rh(I)-PMO-3D catalyst, we studied the 1,4-conjugate addition reaction of different arylboronic acids with *N*,*N*-acrylic amide. The results were presented in Table 2. Both the electron-rich and the electron-deficient arylboronic acids gave desirable products in high yields.

Because the Rh(I)-PMO-3D-2 exhibited good catalytic activity, it is necessary to make sure whether the heterogeneous Rh(I) anchored on the support or homogeneous Rh(I) leached from the support was the real catalyst. The following experiments were carried out according to the procedure proposed by Sheldon et al. (*25*). When the conversion in reaction reached

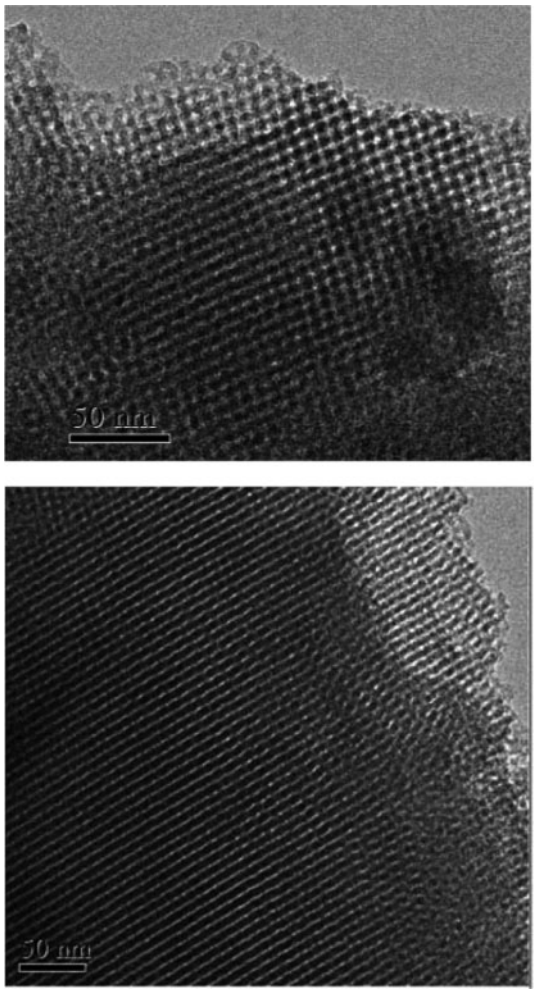

Figure 4. TEM image of the Rh(I)-PMO-3D sample.

30%, the water-medium 1,4-conjugate addition reaction mixture was filtered to remove the solid catalyst, and then the mother liquor was allowed to react for another 7 h under the same reaction conditions. No significant change in either the conversion or the yield of product was observed, which indicated that the active phase was not the Rh(I) species leached from the supports. Therefore, it is reasonable to conclude that the present catalysis was really heterogeneous in nature.

Figure 5 shows the recycling test of the Rh(I)-PMO-3D catalyst in water-medium reaction. No significant decrease in catalytic efficiencies were observed for the Rh(I)-PMO-3D catalyst within five recycles. The excellent durability of the Rh(I)-PMO-3D catalyst could be attributed to the strong interaction of the Rh(I)

Table 2. Rh(I)-PMO-3D-2-catalyzed 1,4-conjugate addition reaction between different arylboronic acids with *N*,*N*-acrylic amide.[a]

R	Reaction time (h)	Conv. (%)	Yield (%)
H	7	95	95
OCH_3	7	94	94
CH_3	7	91	91
Cl	9	89	89
CF_3	9	84	84

[a]Reaction conditions: 0.50 mmol of arylboronic acids, 0.10 mmol of *N*,*N*-acrylic amide, 1.0 mL of toluene, 4.0 mL H_2O, *n*-decane as an internal standard, and a catalyst containing 0.0065 mmol Rh(I), 80°C.

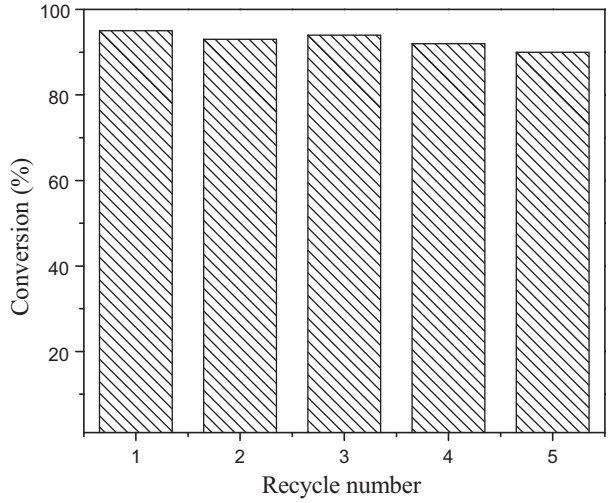

Figure 5. Recycling test of Rh(I)-PMO-3D.

Table 1. Structural parameters and catalytic performances of different catalysts.[a]

Catalyst	S_{BET} ($m^2 \cdot g^{-1}$)	V_P ($cm^3 \cdot g^{-1}$)	D_P (nm)	Rh loading (wt%)	Conv. (%)
None				/	0
$Rh(PPh_3)_3Cl$	/	/	/	/	94
PMO-3D	688	0.67	7.4	0	0
Rh(I)-PMO-2D	677	0.64	7.2	0.87	89
Rh(I)-PMO-3D-1	654	0.71	7.4	0.44	87
Rh(I)-PMO-3D-2	639	0.70	7.2	0.86	95
Rh(I)-PMO-3D-3	655	0.68	7.1	1.1	90

[a]Reaction conditions: 0.50 mmol of phenylboronic acid, 0.10 mmol of *N*,*N*-acrylic amide, 1.0 mL of toluene, 4.0 mL H_2O, *n*-decane as an internal standard, and a catalyst containing 0.0065 mmol Rh(I), 80°C, 7 h.

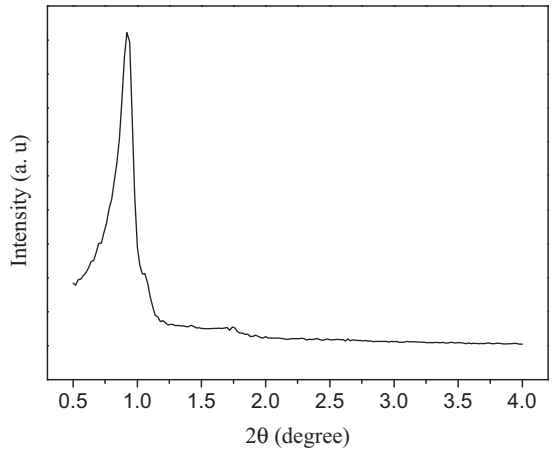

Figure 6. The small-angle XRD pattern of the Rh(I)-PMO-3D sample after being reused five times.

organometallic complex with the organosilica support, which could effectively inhibit the Rh(I)leaching. According to the ICP analysis, Rh(I) species in the solution was less than 0.5 ppm after being used for five times, suggesting that the Rh(I)-leaching could be essentially neglected. In addition, the Rh(I)-PMO-3D catalyst also exhibited strong hydrothermal stability. As shown in Figure 6, the XRD pattern clearly demonstrated that the Rh(I)-PMO-3D remained well-defined ordered mesoporous structure after being reused for five times.

Conclusion

In summary, this work developed a facile approach to synthesize a 3D periodic mesoporous Rh(I) organometalsilica catalyst with both the Rh(I) organometals and the phenyl groups integrally incorporated into the silica walls. During water-medium 1,4-conjugate addition reaction, the Rh(I)-PMO-3D exhibited higher activity than the Rh(I)-PMO-2D and comparable catalytic efficiencies with the corresponding Rh(I)$(PPh_3)_3Cl$ homogeneous catalyst. Remarkably, Rh(I)-PMO-3D could be used repetitively for more than five times without significant deactivation, which offers opportunities for industrial applications of water-medium clean organic reactions.

Funding

This work was supported by the National Natural Science Foundation of China (20825724), the Project from College Natural science research plan of Jiangsu province (13KJB150008), Industrial support plan of Huaian city (HAG2013077), and First Class of China Postdoctoral Science Foundation.

References

(1) Sakai, M.; Hayashi, H.; Miyaura, N. *Organometallics*. **1997**, *16*, 4229.
(2) Sibi, M.P.; Manyem, S. *Tetrahedron*. **2000**, *56*, 8033.
(3) Zhang, S.; Gangal, G.; Uludağ, H. *Chem. Soc. Rev*. **2007**, *36*, 507.
(4) Sheldon, R.; Arends, I.; Hanefeld, U. *Green Chemistry and Catalysis*; Wiley-VCH: Weinheim, **2007**.
(5) Bianchini, G.; Scarso, A.; Chiminazzo, A.; Sperni, L.; Strukul, G. *Green Chem*. **2013**, *15*, 656.
(6) Li, C.J.; Chan, T.H. *Organic Reactions in Aqueous Media*; Wiley: New York, NY, 1997.
(7) Lindstrom, U.M. *Chem. Rev*. **2002**, *102*, 2751.
(8) Yang, X.S.; Zhu, F.X.; Huang, J.L.; Zhang, F.; Li, H. X. *Chem. Mater*. **2009**, *21*, 4925.
(9) Huang, J.L.; Zhu, F.X.; He, W.H.; Zhang, F.; Wang, W.; Li, H.X. *J. Am. Chem. Soc*. **2010**, *132*, 1492.
(10) Guo, W.P.; Kleitz, F.; Choab, K.; Ryoo, R. *J. Mater. Chem*. **2010**, *20*, 8257.
(11) Tan, X.H.; Shen, B.; Deng, W.; Zhao, H.; Guo, Q.X. *J. Org. Lett*. **2003**, *5*, 1833.
(12) Shimazu, S.; Baba, N.; Ichikuni, N.; Uematsu, T.J. *Mol. Catal. A*. **2002**, *182*, 343.
(13) Zhou, J.; Zhou, R.; Mo, L.; Zhao, S.; Zheng, X. *J. Mol. Catal*. **2002**, *178*, 289.
(14) Wan, Y.; Zhang, D.Q.; Feng, C.M.; Chen, J.; Li, H.X. *Chem. An. Asian J*. **2007**, *2*, 875.
(15) Li, H.X.; Zhang, F.; Wan, Y.; Lu, Y.F. *J. Phys. Chem. B*. **2006**, *110*, 22942.
(16) Li, H.X.; Xiong, M.W.; Zhang, F.; Huang, J.L.; Chai, W. *J. Phys. Chem. C*. **2008**, *112*, 6366.
(17) Li, H.X.; Zhang, F.; Yin, H.; Wan, Y.; Lu, Y.F. *Green Chem*. **2007**, *9*, 500.
(18) Krcher, O.; Kppel, R.A.; Frba, M. *J. Catal*. **1998**, *178*, 284.
(19) Burleigh M.; Michael, A.; Markowitz, M.; Spector, S.; Gaber, B.; *J. Phys. Chem. B*. **2001**, *105*, 9935.
(20) Inagaki, S.; Guan, S.; Ohsuna, T.; Terasaki, O. *Nature*. **2002**, *416*, 304.
(21) Simon, P.F.; Ulrich, W.R.; Spiess, H.W.; Wiesner, U. *Chem. Mater*. **2001**, *13*, 3464.
(22) Moulder J.F.; Stickle W.F.; Sobol P.E.; Bomben K. D. *Handbook of X-ray Photoelectron Spectroscopy, A Reference Book of Standard Spectra for Identification and Interpretation of XPS Data*, Perkin-Elmer Corporation, Physical Electronics Division: Eden Prairie, MN, **1992**, p. 183.
(23) Zhao, D.Y.; Huo, Q.; Feng, J.; Chmelka, B.F.; Stucky, G.D., *J. Am. Chem. Soc*. **1998**, *120*, 6024
(24) Cho, E.; Kim, D.; Gorkab, J.; Jaroniec, M. *J. Mater. Chem*. **2009**, *19*, 2076.
(25) Sheldon, R.A.; Wallau, M.I.; Arends, W.C.E.; Schuchardt, U. *Acc. Chem. Res*. **1998**, *31*, 485.